Probing the anisotropic local Universe and beyond with SNe Ia data

Jacques Colin, Roya Mohayaee, Subir Sarkar, Arman Shafieloo

Monthly Notices
of the
ROYAL ASTRONOMICAL SOCIETY

Mon. Not. R. Astron. Soc. **414,** 264–271 (2011) doi:10.1111/j.1365-2966.2011.18402.x

Probing the anisotropic local Universe and beyond with SNe Ia data

Jacques Colin,[1] Roya Mohayaee,[1] Subir Sarkar[2] and Arman Shafieloo[2,3]★

[1]*UPMC, CNRS, Institut d'Astrophysique de Paris, 98 bis Bd. Arago, Paris 75014, France*
[2]*Rudolf Peierls Centre for Theoretical Physics, University of Oxford, 1 Keble Road, Oxford OX1 3NP*
[3]*Institute for the Early Universe, Ewha Womans University, Seoul 120-750, South Korea*

Accepted 2011 January 20. Received 2011 January 20; in original form 2010 December 11

ABSTRACT

The question of the transition to global isotropy from our anisotropic local universe is studied using the Union 2 catalogue of Type Ia supernovae (SNe Ia). We construct a 'residual' statistic sensitive to systematic shifts in their brightness in different directions and use this to search in different redshift slices for a preferred direction on the sky in which the SNe Ia are brighter or fainter relative to the standard Λcold dark matter (ΛCDM) cosmology. At low redshift ($z < 0.05$), we find that an isotropic model such as ΛCDM is barely consistent with the SNe Ia data at 2σ–3σ. A maximum-likelihood analysis of peculiar velocities confirms this finding – there is a bulk flow of 260 km s^{-1} extending out to $z \sim 0.06$, which disagrees with ΛCDM at 1σ–2σ. Since the Shapley concentration is believed to be largely responsible for this bulk flow, we make a detailed study of the infall region: the SNe Ia falling away from the Local Group towards Shapley are indeed significantly dimmer than those falling towards us on to Shapley. Convergence to the CMB rest frame must occur well beyond Shapley ($z > 0.06$) so this low-redshift bulk flow will systematically bias any reconstruction of the expansion history of the Universe. At higher redshifts $z > 0.15$ the agreement between the SNe Ia data and the ΛCDM model does improve, however, the sparseness and low quality of the data mean that the latter cannot be singled out as the preferred cosmological model.

Key words: cosmic background radiation – cosmological parameters – cosmology: theory – dark energy – large-scale sctructure of Universe.

1 INTRODUCTION

Modern cosmology is founded on the cosmological principle which assumes that the Universe is homogeneous and isotropic. The local Universe is, however, observed to be anisotropic and inhomogeneous, exhibiting the 'cosmic web' of voids and superclusters. This presumably causes the Local Group of galaxies move towards a preferred direction $\ell = 276^\circ \pm 3^\circ, b = 30^\circ \pm 2^\circ$ at 627 ± 22 km s^{-1}, as inferred from the dipole anisotropy of the cosmic microwave background (CMB) radiation (Kogut et al. 1993).

On the other hand, the overall isotropy of the CMB (barring the dipole anisotropy due to our local motion) provides strong evidence for an isotropic universe on very large scales.[1] Where does the transition between these two regimes occur? While high-quality data exist at low redshifts and the CMB provides reliable information at very high redshifts, the data are rather sparse and mainly of poor quality on the intermediate scales of interest. Here the SNe Ia Hubble diagram is the key source of information, and so we use the comprehensive Union 2 catalogue (Amanullah et al. 2010) to investigate these important questions.

SNe Ia data have been examined previously to test the isotropy of the Universe (Kolatt & Lahav 2001; Bonvin, Durrer & Kunz 2006; Gordon, Land & Slosar 2007; Schwarz & Weinhorst 2007; Gupta, Saini & Laskar 2008; Koivisto & Mota 2008a,b; Blomqvist, Enander & Mortsell 2008; Cooray, Holz & Caldwell 2010; Gupta & Saini 2010; Koivisto et al. 2011) and to determine whether the Universe accelerates differently in different directions. Recently, a marginal (1σ) detection of anisotropy has been reported on spatial scales where dark energy becomes important (Cooke & Lynden-Bell 2010; Antoniou & Perivolaropoulos 2010). Clearly, better-quality and more complete surveys are needed before any firm conclusions can be drawn. However, although these detections are not significant by themselves, a puzzling and perhaps accidental

★E-mail: arman@ewha.ac.kr

[1] The *WMAP* observations of anomalies in large-angle anisotropies in the CMB, e.g. the hemispherical asymmetry (Eriksen et al. 2004) and the unexpected quadrupole–octupole alignment (de Oliveira-Costa et al. 2004), have led many to question whether the CMB is indeed statistically isotropic (e.g. Copi et al. 2007). However, others have argued that these anomalies may simply be due to the manner in which the galactic foreground was masked (Pontzen & Peiris 2010). We look to forthcoming observations by *Planck* to resolve this contentious issue.

feature is the alignment of the detected anisotropy with the CMB dipole direction. In this work, we demonstrate that the alignment at low redshift is due to the attraction of huge structures such as the Shapley supercluster. At high redshift, the alignment seems to become statistically insignificant but given the sparse and poor-quality data, no strong conclusions can be drawn.

On small scales, the CMB dipole and the bulk flow are aligned, which is unsurprising as the common source of both these motions is very likely the anisotropic distribution of matter in the local Universe. However, a bulk flow much larger than expected has been found extending out to at least 120 Mpc (Watkins, Feldman & Hudson J 2009; Lavaux et al. 2010),[2] which is a $\sim 2\sigma$–3σ fluctuation in a Λcold dark matter (ΛCDM) model since convergence to the CMB rest frame ought to occur at much smaller scales in this model. At low redshifts, we study the bulk flow using two different methods: first by a method of 'smoothing and residuals' (Sections 3 and 4) and secondly by a maximum likelihood analysis (Section 5). We show that these two methods are in good agreement at small redshifts ($z < 0.05$) and confirm that there is indeed a discrepancy between the ΛCDM model prediction for the bulk flow and the SNe Ia observations.

The Shapley concentration at $z \simeq 0.035$–0.055 is believed to be the main source of our large bulk motion. We study the infall region around Shapley (Section 6) and demonstrate that SNe Ia beyond Shapley are systematically brighter than expected in an isotropic universe (as they are falling towards Shapley), while SNe Ia between the Local Group and Shapley are systematically dimmer (as they are also falling towards Shapley, but away from us). This result is obtained using our smoothing and residuals scheme.

At high redshift, the χ^2 statistic cannot be used since the bulk flow becomes small relative to the Hubble expansion rate. Using the method of smoothing and residuals for $z > 0.05$ we find that an isotropic model such as ΛCDM is consistent with the data. However, the poor quality of the data means that anisotropic models cannot be eliminated.

Since the high-redshift results may be contaminated by the low-redshift data, we perform a 'cosmic tomography' – the data are sliced up in redshift and the question of isotropy is studied separately for each slice. The differential analysis is then complemented by a cumulative analysis to establish the correlation between different shells. We present our conclusions in Section 7.

2 THE UNION 2 SUPERNOVAE CATALOGUE

The Union 2 catalogue (Amanullah et al. 2010) contains 557 SNe Ia of which 165 are at $z < 0.1$. This is the largest compilation of SNe Ia to date from several different surveys including Union (Kowalski et al. 2008), CfA (Hicken et al. 2009) and Sloan Digital Sky Survey (SDSS) (Kessler et al. 2009), in addition to data on six new SNe Ia reported by Amanullah et al. (2010). While efforts have been made to obtain good control over the systematics, it is recognized that combining data from different surveys can introduce additional biases. Nevertheless, this is the best data set available at present.

In Fig. 1, we illustrate by the size of the spots the discrepancy between the luminosity distance of Union 2 SNe Ia and the value predicted by the standard ΛCDM model, for $z < 0.06$ (top panel) and $z > 0.06$ (middle panel). The red spots indicate SNe Ia further away than the ΛCDM prediction, while the green spots indicate those which are closer. In the bottom panel of Fig. 1 the size of the spots represents the observational uncertainties. We note that there

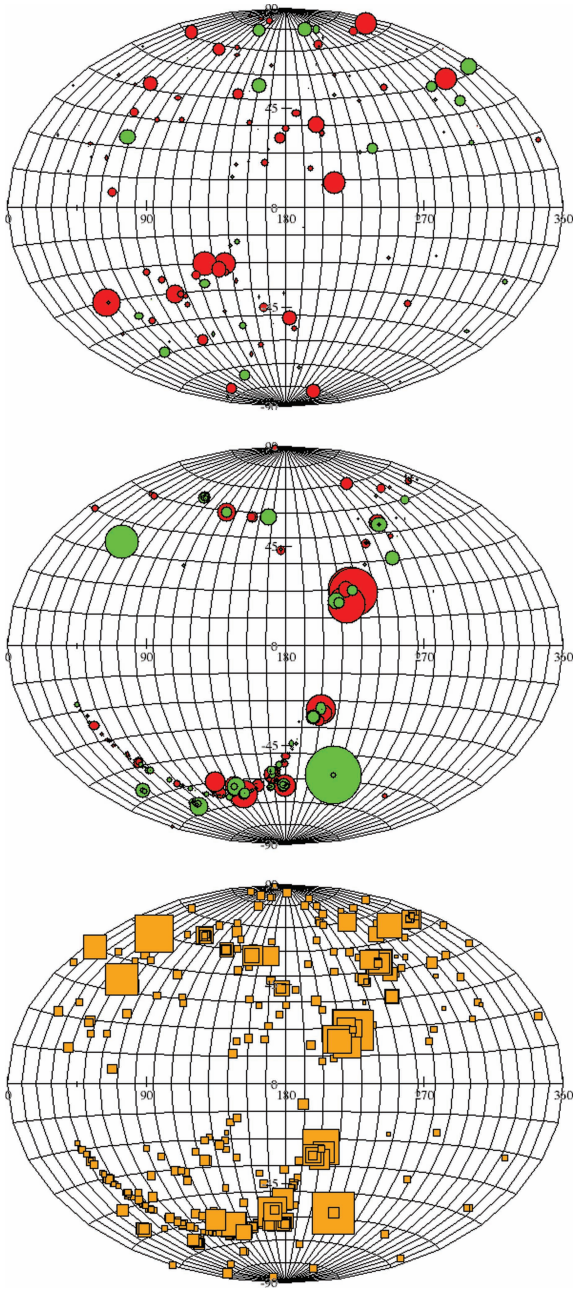

Figure 1. Top panel: Aitoff–Hammer presentation of the Union 2 data for $z < 0.06$. The red spots represent the data points with distance moduli, $\mu_{\rm data}$, larger than the values, $\mu_{\Lambda{\rm CDM}}$, predicted by ΛCDM and the green spots are those with $\mu_{\rm data} < \mu_{\Lambda{\rm CDM}}$; the spot size is a relative measure of the discrepancy. A dipole anisotropy is visible around the direction $b = -30^\circ$, $\ell = 96^\circ$ (red points) and its opposite direction $b = 30^\circ$, $\ell = 276^\circ$ (small green points), which is the direction of the CMB dipole. The middle panel is the same plot for $z > 0.06$. The data seem to be homogeneously distributed at small redshifts but suffers from a significant selection effect at large redshifts. The bottom panel shows the full Union 2 data set ($0.015 < z < 1.5$) but now the size of the spots corresponds to the observational uncertainties – a clear correlation is seen with the model-data discrepancy.

[2] Kashlinsky et al. (2008, 2010) have reported an even faster coherent flow out to at least ~800 Mpc, using measurements of the kinematic Sunyaev–Zeldovich effect in galaxy clusters.

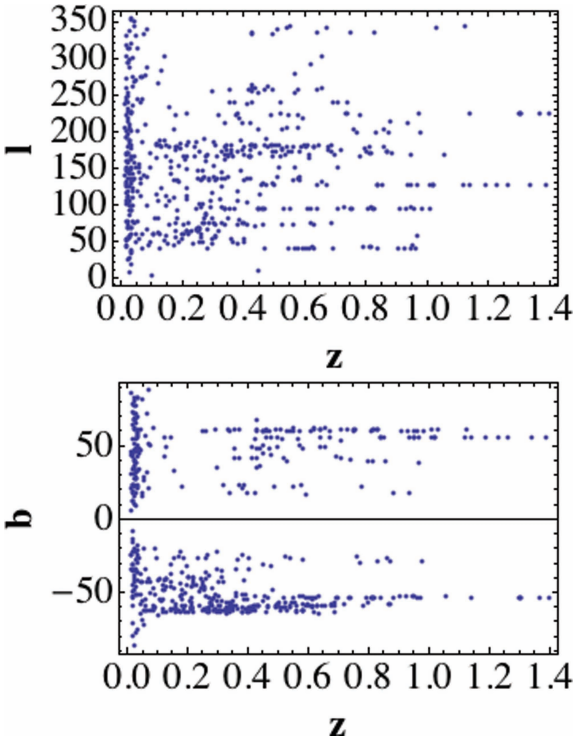

Figure 2. The distribution in galactic longitude (ℓ) and latitude (b) of the Union 2 SNe Ia, as a function of the redshift z. At high redshift, there are significant selection effects and it is difficult to draw any definite conclusions about the anisotropy of the Universe; however at small redshift ($z < 0.06$) the data are quite homogeneous and robust tests of local anisotropy can be made.

is a clear correlation between the latter and the discrepancy between the luminosity distances and the ΛCDM model.

As seen in Fig. 2, the data are quite homogeneously distributed over the sky at redshifts $z < 0.06$; however at higher redshifts the data become increasingly sparse.

3 THE METHOD OF RESIDUALS

If the assumption of the isotropy of the Universe is correct then any residuals remaining from the subtraction of the isotropic model from the data should be distributed randomly around zero (assuming the systematics are under control). In this work, we fit the standard ΛCDM model to the Union 2 data (Amanullah et al. 2010), subtract the best-fitting model from the data and then build a statistic to analyse the residuals. This analysis involves the following steps.

First, we consider an $H(z)$ parametrization (viz. ΛCDM) and a set of SNe Ia data $\mu_i(z_i, \theta_i, \phi_i)$ – we choose to use galactic coordinates (ℓ, b) for θ_i, ϕ_i. At low redshifts $z \ll 1$, the Hubble law implies a linear relationship between distance and redshift so the choice of cosmological model is irrelevant; however this becomes important at high redshift.

Secondly, we obtain the best-fitting form of $\tilde{H}(z)$ and the corresponding best-fitting distance moduli $\tilde{\mu}(z)$, then construct the error-normalized difference of the data from the model,

$$q_i(z_i, \theta_i, \phi_i) = \frac{\mu_i(z_i, \theta_i, \phi_i) - \tilde{\mu}_i(z_i, \theta_i, \phi_i)}{\sigma_i(z_i, \theta_i, \phi_i)} , \quad (1)$$

as in previous work (Perivolaropoulos & Shafieloo 2009; Shafieloo, Clifton & Ferreira 2010). Here, $\mu_i(z_i, \theta_i, \phi_i)$ and $\sigma_i(z_i, \theta_i, \phi_i)$ represent the distance modulus and the relative error bar of the i'th data point, and $\tilde{\mu}_i(z_i, \theta_i, \phi_i)$ is the expected distance modulus in the assumed theoretical model at z_i. Henceforth, we work with these residuals, $q_i(z_i, \theta_i, \phi_i)$, and consider their angular distribution on the sky.

Thirdly, we define a measure $Q(\theta, \phi)$ on the surface of a sphere of unit radius using these residuals:

$$Q(\theta, \phi) = \sum_{i=1}^{N} q_i(z_i, \theta_i, \phi_i) W(\theta, \phi, \theta_i, \phi_i) , \quad (2)$$

where N is the number of SNe Ia data points and $W(\theta, \phi, \theta_i, \phi_i)$ is a weight function (or window function) in our 2D smoothing over the surface of the sphere. We define this weight by the Gaussian distribution:

$$W(\theta, \phi, \theta_i, \phi_i) = \frac{1}{\sqrt{2\pi}\delta} \exp\left[-\frac{L(\theta, \phi, \theta_i, \phi_i)^2}{2\delta^2}\right] , \quad (3)$$

where δ is the width of smoothing and $L(\theta, \phi, \theta_i, \phi_i)$ is the distance on the surface of a sphere of unit radius between two points with spherical coordinates (θ, ϕ) and (θ_i, ϕ_i):

$$L(\theta, \phi, \theta_i, \phi_i) = 2 \arcsin \frac{R}{2} , \quad (4)$$

where

$$R = \big([\sin(\theta_i)\cos(\phi_i) - \sin(\theta)\cos(\phi)]^2 + [\sin(\theta_i)\sin(\phi_i) - \sin(\theta)\sin(\phi)]^2 + [\cos(\theta_i) - \cos(\theta)]^2\big)^{1/2} .$$

Thus, any anisotropy in the data in any specific direction will translate into $Q(\theta, \phi)$ being significantly less or more than zero, depending on the quality of the data.

Finally, we adopt a value for δ, calculate $Q(\theta, \phi)$ on the whole surface of the sphere and find the minimum and maximum of this quantity, $Q(\theta_{\min}, \phi_{\min})$ and $Q(\theta_{\max}, \phi_{\max})$. Our statistical measure of anisotropy is based on the difference

$$\Delta Q_{\rm data} = Q(\theta_{\max}, \phi_{\max}) - Q(\theta_{\min}, \phi_{\min}), \quad (5)$$

i.e. a large value of $\Delta Q_{\rm data}$ implies significant anisotropy. To estimate the significance, we simulate 1000 realizations of the data with the same angular positions on the sky and the same error bars (assuming a Gaussian distribution), determine ΔQ_j and then do a simple test to determine the significance of our results for the real data. Any anisotropy in the SNe Ia sample would be more significant if $\Delta Q_{\rm data}$ is *larger* than most of ΔQ_js for the simulated data. From the resulting frequency distribution of this statistic one can derive a *P*-value, defined as the probability that, given the null hypothesis, the value of the statistic is larger than the one observed. We remark that in defining this statistic one has to be cautious about *a posteriori* interpretations of the data; a particular feature observed in the real data may be very unlikely, but the probability of observing *some* feature may be quite large – see Spergel et al. (2003), Lewis (2003) and the discussion in Hamann, Shafieloo & Souradeep (2010).

We would like to point out here some additional advantages of our method. First, the only parameter in this analysis is the value of δ – the width of Gaussian smoothing on the surface of the 2D sphere. Its value cannot affect the results when testing the consistency of the data with an isotropic universe, since we are dealing only with the residuals and the real data are compared with its simulated samples in exactly the same manner. Secondly, the isotropy of the data can be checked in a completely *model-independent* manner and the significance of the findings can also be checked to avoid any misinterpretation of the data. Thirdly, the method is able to detect anisotropy even in small patches of the sky if there is sufficient data available. In fact, our method is not limited to finding only dipoles in

the sky but can be useful if there is a neighbouring local void or any unexpected bulk flow up to modest redshifts in a specific direction. Moreover, because of working with the normalized residuals, the method is insensitive to those regions of the sky where there is no data, which makes it relatively bias-free. Hence, it is particularly suitable for $z > 0.05$ where there are rather few data points. Although in this analysis we focus on the isotropic model of the universe, our method can be used to test any other model, in particular anisotropic models.

We wish to emphasize the difference between testing the consistency of a cosmological model with the data, and finding the model that best describes the Universe. Depending on the quality, quantity and distribution of the data there may be several (degenerate) models that are all consistent with the data. For example, we may find that the isotropic model of universe fits the data, but that the data are so sparse at high redshifts that in many patches of the sky we do not have even a single data point, so an anisotropic model which has features in these directions can also fit the data.

4 TEST OF ISOTROPY USING THE METHOD OF RESIDUALS

We now use the method of smoothing and residuals to test the isotropy of the Universe using SNe Ia data at different redshifts and for different values of the smoothing parameter δ. We divide the Union 2 data (Amanullah et al. 2010) into five bins at $z < 0.1$ and seven bins at $z > 0.1$ so as to have sufficient number of data points in each bin (see Table 1). In each case the real data are compared with the results from 1000 Monte Carlo realizations assuming an isotropic universe. The underlying cosmological model is assumed to be a flat ΛCDM model with $\Omega_{0\mathrm{m}} = 0.27$ (which is very close to the best-fitting flat ΛCDM model for Union 2 data).

In Fig. 3, we show results for the first three low-redshift shells and the cumulative result when data in all three shells are combined. Although each individual shell is reasonably consistent with isotropy, combining the data indicates an inconsistency of the ΛCDM model with the data at $>2\sigma$. This happens because the direction of the mild anisotropy in all three shells points the same way.

We have added Table 2 to emphasize that the important quantity at low-z is not the P-value alone, since similar P-values are obtained also at high redshift. One should consider also the *consistency* of adjacent shells: the anisotropy in the first three shells point towards nearly the same direction. This strong correlation makes the P-value for the cumulative result of the first three shells rather low: $z = 0.045$. Fig. 3 and Table 2 show that at $z > 0.1$ there are no adjacent shells that point towards the same direction, hence, the effect of these shells at high redshift cancel each other in the cumulative result and the effect of the first three shells dominates. The importance of our differential shell analysis is now evident – any anisotropy in some specific redshift range would be smoothed out if one were to use only the whole data set.

It is also possible to look for dipoles in different shells using our method. We look for a direction in the sky for which the value of ΔQ between that point (ℓ, b) and its opposite point on the surface of the sphere – i.e. $(\ell + 180, -b)$ if $\ell < 180$ and $(\ell - 180, -b)$ if $\ell > 180$ – is maximum. To calculate dipoles in different shells we set $\delta = \pi/2$; for this value the weighted average using Gaussian smoothing is almost identical to the weighted average by the inner product (i.e. $\cos\theta$) that is usually used to find dipoles.

In Fig. 4, we see the positions of the dipoles in galactic coordinates for different redshift shells. The size of the spots is proportional to the P-values that are derived by comparing the results from the real data to the 1000 Monte Carlo realizations of the data when the assumed model is ΛCDM. Bigger spots indicate a more anisotropic behaviour or lower level of agreement between ΛCDM and the real data (the size of the spots is proportional to the P-value). In the bottom panel we see the cumulative results which can help us to identify correlations between neighbouring shells.

In Table 2, we see these results for different shells, both individual and cumulative. It is interesting to see that the P-value drops to 0.014 at $z < 0.045$, i.e. a clear inconsistency between ΛCDM (i.e. isotropy) and the data. The P-value increases again with increasing redshift, suggesting that we are approaching the CMB rest frame. This can be seen more clearly by looking at the top panel of Fig. 5 where P-values are plotted versus redshift for different cumulative shells. In the bottom panel of Fig. 5 we can see the results from our residuals analysis where we have divided the data into two subsamples – one for low redshifts $0.015 < z < 0.06$ and another for higher redshifts $0.15 < z$. At small redshifts, the isotropic universe lies over σ away from the data with $P = 0.054$ for $0.015 < z < 0.06$. However, at higher redshift this discrepancy drops to $\sim 1\sigma$ with $P = 0.594$ for $z > 0.15$.

5 TEST OF ISOTROPY AND LOCAL BULK FLOW USING MAXIMUM LIKELIHOOD ANALYSIS

Now we use a different method to examine the low-redshift anisotropy detected above. We assume a bulk flow and use the maximum likelihood analysis method to find its value (Riess, Press & Kirsher 1995, 1996). We consider SNe Ia at $z < 0.06$ (since the bulk flow would be negligible in relation to the Hubble expansion rate at higher redshift) and minimize, for the Union 2 data:

$$\chi^2(\Omega_{0\mathrm{m}}, V_{\mathrm{bulk}}, j(\ell, b)) = \sum_{i=1}^{N} \frac{\left[\mu_i^{\mathrm{Union2}} - 5\log_{10}\left(d_{\ell_i}^{\Lambda\mathrm{CDM}}(\Omega_{0\mathrm{m}}, H_0) + \frac{V_{\mathrm{bulk}}\cdot j(\ell,b)}{H_0}\right) - 25\right]^2}{\sigma_i^2}, \quad (6)$$

where N is the number of SNe Ia, $j(\ell, b)$ is a unit vector representing the direction on the sky in Galactic coordinates, V_{bulk} is the local bulk flow velocity in km s^{-1}, $d_{\ell_i}^{\Lambda\mathrm{CDM}}(\Omega_{0\mathrm{m}}, H_0)$ is the luminosity distance for the standard flat ΛCDM model and $\Omega_{0\mathrm{m}}$ is the present-day matter density (set equal to 0.27 although the choice is not important since the Hubble law is linear here). It should be noted that in dealing with SNe Ia data, H_0 is treated as a 'nuisance parameter'. We consider different cumulative redshift slices of the data, viz. $0.015 < z < 0.025$, $0.015 < z < 0.035$, $0.015 < z < 0.045$ and $0.015 < z < 0.06$.

Table 1. Number of SNe Ia per redshift bin in the Union 2 catalogue.

Δz	0.015–0.025	0.025–0.035	0.035–0.045	0.045–0.06	0.06–0.1	0.1–0.2
N	61	48	18	15	23	55
Δz	0.2–0.3	0.3–0.4	0.4–0.5	0.5–0.6	0.6–0.8	0.8–1.4
N	62	63	58	43	51	60

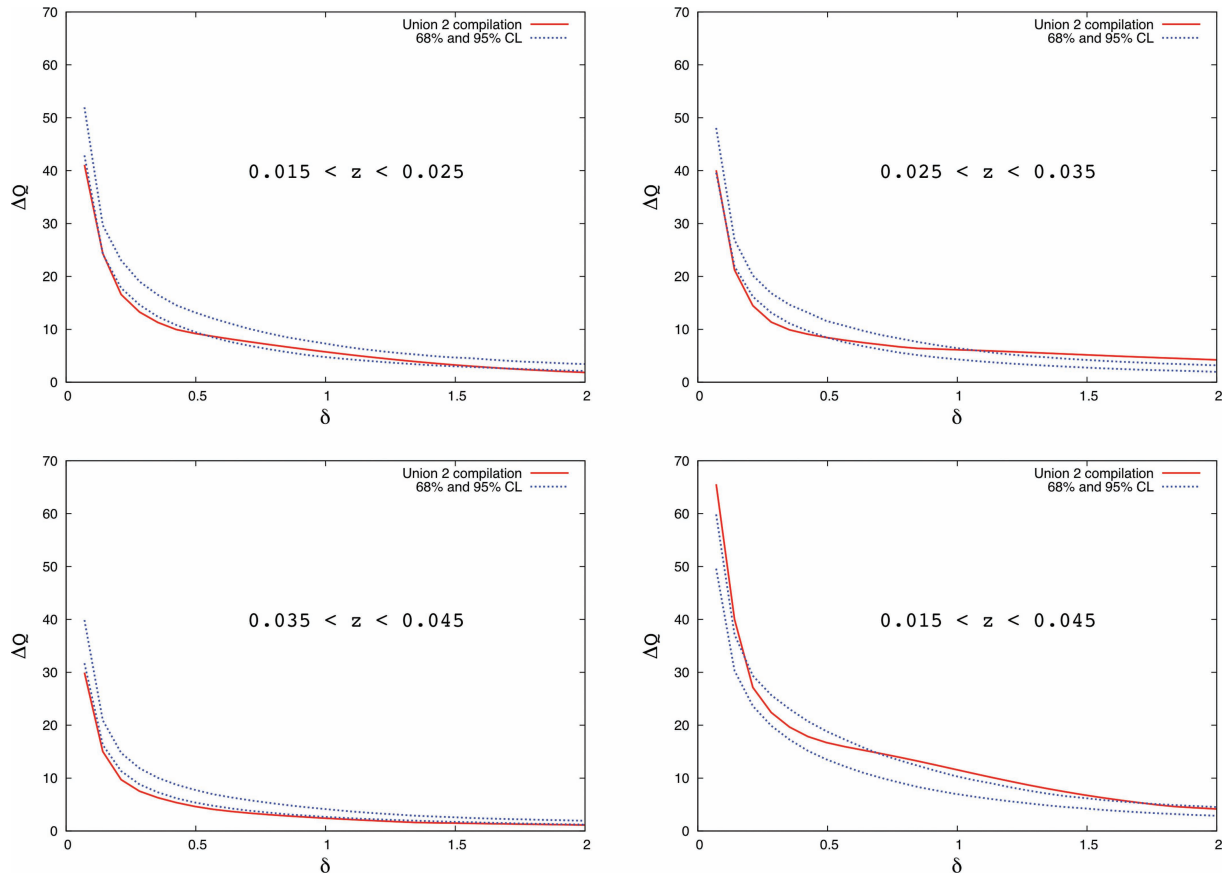

Figure 3. The anisotropy measure ΔQ (equation 5) plotted against the smoothing length δ, for different redshift shells. The full (red) lines show the results for the Union 2 SNe Ia data and the dotted (blue) lines are 68 per cent and 95 per cent confidence limits derived from 1000 Monte Carlo realizations. While each individual shell is consistent with isotropy, all shells have a mild anisotropy in the same direction so the cumulative result from combining them is inconsistent with isotropy at over 2σ, as seen in the lower right panel.

Table 2. Results from the residuals analysis for the *P*-value which quantifies the level of agreement between the isotropic universe and the data, for shells in redshift. On the left are the results for the individual shells and on the right for the cumulative shells.

Δz	b°	ℓ°	*P*-value	Δz	b°	ℓ°	*P*-value
0.015–0.025	46	265	0.140	0.015–0.025	46	265	0.140
0.025–0.035	2	320	0.112	0.015–0.035	27	297	0.039
0.035–0.045	20	312	0.354	0.015–0.045	26	300	0.014
0.045–0.06	−46	65	0.267	0.015–0.06	19	309	0.054
0.06–0.1	−41	75	0.637	0.015–0.1	14	316	0.153
0.1–0.2	−3	219	0.608	0.015–0.2	13	299	0.265
0.2–0.3	29	21	0.602	0.015–0.3	20	314	0.226
0.3–0.4	−83	348	0.854	0.015–0.4	10	314	0.329
0.4–0.5	70	238	0.428	0.015–0.5	27	307	0.285
0.5–0.6	16	15	0.177	0.015–0.6	27	326	0.180
0.6–0.8	−77	45	0.108	0.015–0.8	3	332	0.279
0.8–1.4	−54	152	0.947	0.015–1.4	−2	332	0.369

In Fig. 6, we see that the data for $0.015 < z < 0.025$ (top panel) fit best with $V_{\rm bulk} = 260$ km s^{-1} in the direction $b = 16^\circ$, $\ell = 271^\circ$ which is close to the direction of the CMB dipole ($b = 30^\circ$, $\ell = 276^\circ$) (Kogut et al. 1993). However, the 1σ contours are quite large and an isotropic local universe with $V_{\rm bulk} = 0$ is also consistent with the data at 2σ. When we assume a bigger cumulative cut, the 1σ and 2σ regions shrink and we can see that the isotropic universe is now shifted outside the 2σ region (Fig. 6, bottom panel). We can observe the same trend up to $0.015 < z < 0.045$ where the 1σ and 2σ regions are still shrinking as seen in Fig. 7 (top panel). However in the next step when we consider the data for $0.015 < z < 0.06$, the 1σ and 2σ regions start becoming larger again (Fig. 7, bottom panel). These results are completely consistent with our results from the smoothing and residuals analysis. So we can conclude that the bulk of the local universe of radius $z \sim 0.05$ is moving towards the CMB dipole direction with $V_{\rm bulk} = 260$ km s^{-1}.

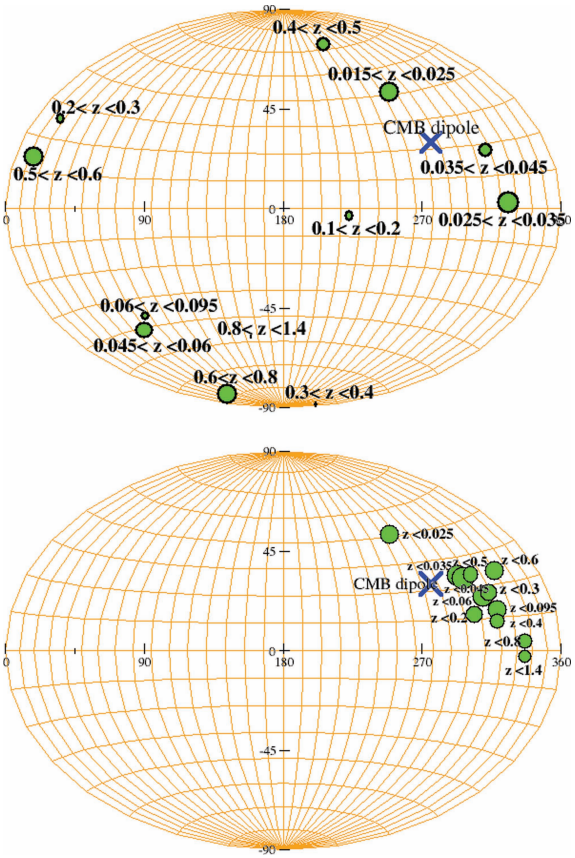

Figure 4. Top panel: the dipole direction found by the residuals method in different redshift shells. Bottom panel: the cumulative dipole direction in shells of increasing radii. The size of the spots is proportional to the *P*-value; larger spots represent more significant disagreement between the data and the ΛCDM model.

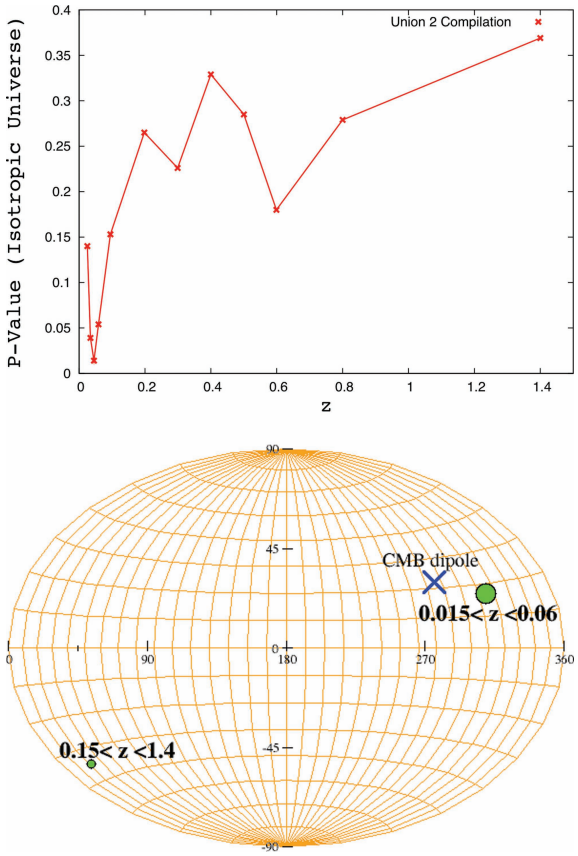

Figure 5. Top panel: *P*-value for the consistency of the isotropic universe with the data versus redshift. At $z \approx 0.05$ the *P*-value drops to 0.014 showing that isotropy is excluded at 3σ and we are not yet in the CMB rest frame. Bottom panel: the cumulative analysis shows that at small redshift isotropy is excluded at 2σ–3σ with $P = 0.054$ for $0.015 < z < 0.06$; however at higher redshift agreement is achieved within 1σ, with $P = 0.594$ for $0.15 < z < 1.4$.

Our results are consistent with Watkins et al. (2009) who estimate a bulk flow of $V_{\rm bulk} = 416 \pm 78\,{\rm km\,s^{-1}}$ towards $b = 60^\circ(+6, -6)$, $\ell = 282^\circ(+11, -11)$ at a scale of $100\,h^{-1}$ Mpc. On this scale we find $V_{\rm bulk} = 250(+190, -160)\,{\rm km\,s^{-1}}$ towards $b = 21^\circ(+34, -52)$, $\ell = 287^\circ(+62, -48)$, i.e. our results are consistent within 1σ.

In Fig. 8, we see that the derived bulk flow using the cumulative SNe Ia data is inconsistent with the prediction of a flat ΛCDM model at 1σ–2σ. This is a slight improvement over using residuals (where the disagreement with ΛCDM was at 2σ–3σ) the reason being that at small redshift one needs to compare the data with the model at first-order in perturbation theory. At high redshifts the comparison can be done directly between the data and the unperturbed model since the perturbations have subsided on large scales.

6 SHAPLEY INFALL

It is generally believed that our local bulk flow is due mainly to the gravitational attraction of the Shapley supercluster which lies at around $z \sim 0.04$ and that beyond Shapley the reference frame should converge to the CMB rest frame. We use the method of smoothing and residuals, discussed in Section 3, to study the infall towards the Shapley concentration. Somewhat surprisingly, the SNe Ia data provide us with a clear picture of the infall.

We take Shapley to have an approximate extension of $0.035 < z < 0.055$. First, we consider all data in the redshift band $0.015 < z < 0.0345$ which contain 109 SNe Ia and evaluate the dipole which, as shown in Fig. 9, points towards Shapley (which is approximately aligned with the direction of the CMB dipole). While the movement towards Shapley seems to be strongly favoured by the data, the *P*-value for the isotropic universe is about $P = 0.039$. Next, we consider the data in the redshift range $0.0522 < z < 0.095$ which contain 32 SNe Ia and as shown in Fig. 9, the direction now becomes completely *opposite*, indicating these SNe Ia are infalling towards Shapley. The *P*-value for the isotropic universe in this range is $P = 0.339$. Thus, future precision SNe Ia data can provide us with valuable information on the formation history of this giant supercluster.

7 CONCLUSIONS

We have used SNe Ia data from the Union 2 catalogue to study the (an)isotropy of our Universe. Since the low- and high-redshift anisotropy can in principle be of different origin, we have analysed the data tomographically in different redshift slices, and also the cumulative data set in order to trace any correlation between different slices. We have developed a statistical tool of 'residuals' to examine the data in an unbiased manner at all redshifts. At low redshift, we have performed a maximum likelihood analysis (which is however unsuitable at high redshift). We find that an isotropic model like ΛCDM is 2σ–3σ away from the data at $z < 0.06$. Although the agreement improves at high redshifts (to within 1σ),

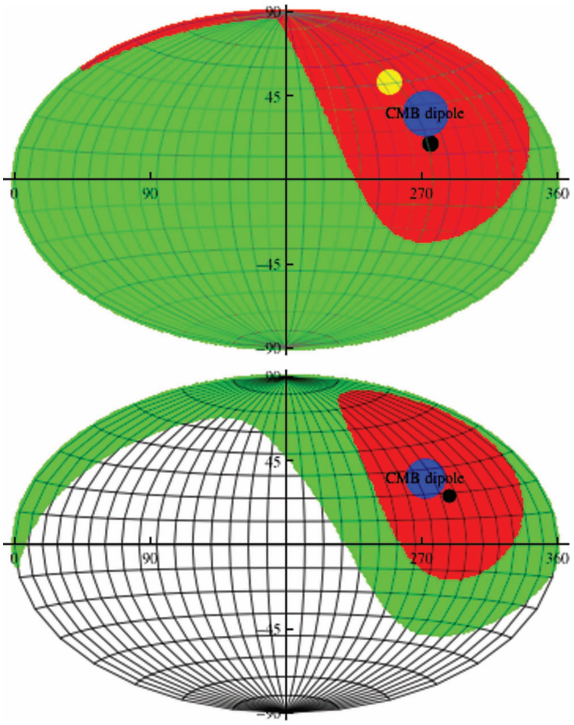

Figure 6. The top panel shows the dipole from the maximum likelihood analysis in the redshift band $0.015 < z < 0.025$ (61 SNe Ia). The best-fitting point is at ($b = 16^\circ$, $\ell = 271^\circ$) for $V_{\rm bulk} = 250$ km s^{-1} and the red and green contours are the 1σ and 2σ confidence regions. The large blue spot is the direction of CMB dipole ($b = 30^\circ \pm 2$, $\ell = 276^\circ \pm 3$). The larger yellow spot, close to the CMB direction, is the best-fitting direction from the residuals analysis and the smaller black spot is the best-fitting direction from the maximum likelihood analysis (the magnitude of the dipole was given in Fig. 8). The bottom panel shows the dipole for the redshift range $0.015 < z < 0.035$ (109 SNe Ia). The blue spot is the CMB dipole and the black spot at $b = 21^\circ$, $\ell = 287^\circ$ is the best fit from the likelihood analysis for $V_{\rm bulk} = 260$ km s^{-1}, while the red and green patches are the 1σ and 2σ confidence regions.

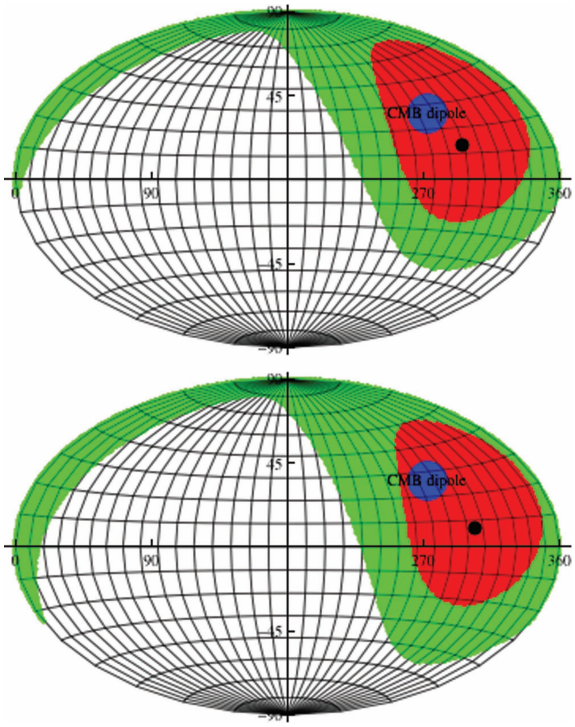

Figure 7. The top panel is for the range $0.015 < z < 0.045$ (127 SNe Ia) and the bottom panel is for $0.015 < z < 0.06$ (142 SNe Ia). The blue spot is the CMB dipole ($b = 30^\circ \pm 2$, $\ell = 276^\circ \pm 3$) and the black spots are the best fit from the likelihood analysis at ($b = 15^\circ$, $\ell = 291^\circ$) for $V_{\rm bulk} = 270$ km s^{-1} for the top panel and at ($b = 8^\circ$, $\ell = 298^\circ$) for $V_{\rm bulk} = 260$ km s^{-1} for the bottom panel, while the red and green patches are the 1σ and 2σ confidence regions.

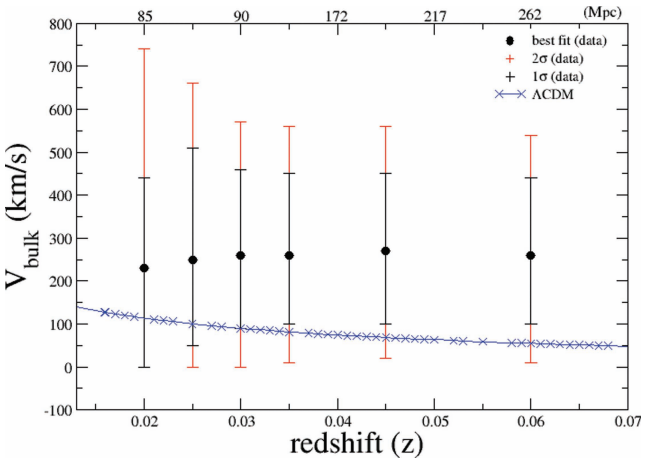

Figure 8. The bulk flow as a function of redshift from the likelihood analysis. We see that a fast flow with $V_{\rm bulk} = 260$ km s^{-1} persists up to at least $z = 0.06$ and systematically exceeds the peculiar velocity expected in ΛCDM (blue line) normalized to *WMAP*-5 parameters (Watkins et al. 2009).

we cannot single out ΛCDM as the preferred model of the Universe. The data become rather sparse at high redshift and the error in distance measures increases, so the data may also agree with alternative anisotropic models.

At low redshift, our results are rather robust and we find a bulk flow of about 260 km s^{-1} in the direction of the Shapley supercluster. We show that the Union 2 data provide the first evidence of the infall on to Shapley; SNe Ia which are falling away from us and towards Shapley are statistically dimmer than those which lie beyond this supercluster and are falling towards us. We see no indication of the decay of the bulk flow after Shapley which suggests that the scale of anisotropy of our local Universe is bigger than is usually assumed and extends beyond $z \sim 0.1$.

Our analysis and results are important for the study of the expansion history of the Universe and the properties of dark energy. In all SNe Ia compilations, an uncertainty of 300–500 km s^{-1} is assumed for each data point to allow for bias introduced by random peculiar velocities. However when there is a *coherent* motion of SNe Ia towards a specific direction, this bias cannot be removed by just increasing the size of the error bar (i.e. assuming the peculiar velocities to be random). We will present in future work the effect of this systematic motion of SNe Ia at low redshifts on the reconstruction of the expansion history of the Universe and estimation of cosmological parameters like $q(z)$, $w(z)$ or 'Om'(z) (Sahni, Shafieloo & Starobinsky 2008; Shafieloo, Sahni & Starobinsky 2009).

We also note the interesting observation by Tsagas (2010) that observers with peculiar velocities have local expansion rates which are appreciably different from the smooth Hubble flow, so can experience *apparently accelerated expansion* when the Universe is actually decelerating. Thus, whether dark energy really needs to be

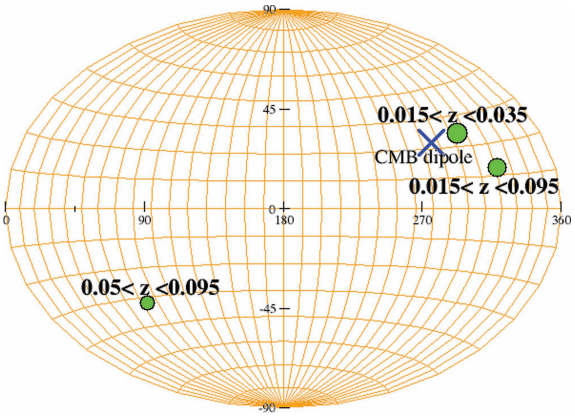

Figure 9. Shapley infall region as probed by the Union 2 SNe Ia data. The region in the redshift band $0.015 < z < 0.0345$ is falling towards Shapley in the direction shown by the big green spot ($P = 0.039$ for the isotropic universe). However, the shell $0.0522 < z < 0.095$ is falling towards Shapley in the opposite direction shown by another green spot ($P = 0.339$ for the isotropic universe). Finally, we show the cumulative result in the range $0.015 < z < 0.095$ – the whole region is still moving in the direction of Shapley, as shown by the green spot ($b = 14^\circ$, $\ell = 316^\circ$, $P = 0.153$). The CMB dipole direction is the large blue cross.

invoked to explain the SNe Ia Hubble diagram and other observations remains an open question (Sarkar 2008).

ACKNOWLEDGMENTS

AS, JC and RM thank the French ANR OTARIE for travel support. AS and SS acknowledge the support of the EU FP6 Marie Curie Research and Training Network 'UniverseNet' (MRTN-CT-2006-035863) and the hospitality of the Institut d'Astrophysique de Paris where part of this work was undertaken. AS acknowledges the support of the Korea World Class University grant no. R32-10130. We thank Mike Hudson, Robert Kirshner and, especially, Leandros Perivolaropoulos for useful discussions and acknowledge the use of the Union 2 data provided by M. Blomqvist, J. Enander and E. Mortsell (Blomqvist, Enander & Mortsell 2010; http://ttt.astro.su.se/ michaelb/SNdata/).

REFERENCES

Amanullah R. et al., 2010, ApJ, 716, 712
Antoniou A., Perivolaropoulos L., 2010, J. Cosmology Astropart. Phys., 12, 012
Blomqvist M., Mortsell E., Nobili S., 2008, J. Cosmology Astropart. Phys., 06, 027
Blomqvist M., Enander J., Mortsell E., 2010, J. Cosmology Astropart. Phys., 10, 018
Bonvin C., Durrer R., Kunz M., 2006, Phys. Rev. Lett., 96, 191302
Cooke R., Lynden Bell D., 2010, MNRAS, 401, 1409
Cooray A., Holz D. E., Caldwell R., 2010, J. Cosmology Astropart. Phys., 11, 015
Copi C., Huterer D., Schwarz D., Starkman G., 2007, Phys. Rev. D., 75, 023507
de Oliveira-Costa A., Tegmark M., Zaldarriaga M., Hamilton A., 2004, Phys. Rev. D., 69, 063516
Eriksen H. K., Hansen F. K., Banday A. J., Gorski K. M., Lilje P. B., 2004, ApJ, 605, 14
Gordon C., Land K., Slosar A., 2007, Phys. Rev. Lett., 99, 081301
Gupta S., Saini T. D., 2010, MNRAS, 407, 651
Gupta S., Saini T. D., Laskar T., 2008, MNRAS, 388, 242
Hamann J., Shafieloo A., Souradeep T., 2010, J. Cosmology Astropart. Phys., 04, 010
Hicken M. et al., 2009, ApJ, 700, 331
Kashlinsky A., Atrio-Barandela F., Kocevski D., Ebeling H., 2008, ApJ, 686, L49
Kashlinsky A., Atrio-Barandela F., Ebeling H., Edge A., Kocevski D., 2010, ApJ, 712, L81
Kessler R. et al., 2009, ApJS, 185, 32
Kogut A. et al., 1993, ApJ, 419, 1
Koivisto T. S., Mota D. F., 2008a, ApJ, 679, 1
Koivisto T. S., Mota D. F., 2008b, J. Cosmology Astropart. Phys., 0806, 018
Koivisto T. S., Mota D. F., Quartin M., Tom G., Zlosnik T. G., 2011, Phys. Rev. D, 83, 023509
Kolatt T. S., Lahav O., 2001, MNRAS, 323, 859
Kowalski M. et al., 2008, ApJ, 686, 749
Lavaux G., Tully R. B., Mohayaee R., Colombi A., 2010, ApJ, 709, 483
Lewis A., 2003, preprint (arXiv:astro-ph/0310186)
Perivolaropoulos L., Shafieloo A., 2009, Phys. Rev. D, 79, 123502
Pontzen A., Peiris H. V., 2010, Phys. Rev. D., 81, 103008
Riess A. G., Press W. H., Kirshner R. P., 1995, ApJ, 445, L91
Riess A. G., Press W. H., Kirshner R. P., 1996, ApJ, 473, 88
Sahni V., Shafieloo A., Starobinsky A. A., 2008, Phys. Rev. D., 78, 103502
Sarkar S., 2008, Gen. Rel. Grav., 40, 269
Schwarz D. J., Weinhorst B., 2007, A&A, 474, 717
Shafieloo A., Sahni V., Starobinsky A. A., 2009, Phys. Rev. D., 80, 101301
Shafieloo A., Clifton T., Ferreira P., 2010, preprint (arXiv:1006.2141)
Spergel D. N. et al., 2003, ApJS, 148, 175
Tsagas C. G., 2010, MNRAS, 405, 503
Watkins R., Feldman H. A., Hudson M. J, 2009, MNRAS, 392, 743

This paper has been typeset from a TEX/LATEX file prepared by the author.